A hybrid Lagrangian-dispersion model for spray drift prediction applied to horizontal boom sprayers

Carlos A. Renaudo [a, b, *], Diego E. Bertin [a, b], Verónica Bucalá [a, b]

[a] *Departamento de Ingeniería Química, Universidad Nacional del Sur (UNS), Argentina*
[b] *Planta Piloto de Ingeniería Química, PLAPIQUI (UNS-CONICET), Bahía Blanca, Argentina*

ARTICLE INFO

ABSTRACT

A spray drift model for horizontal boom sprayers was developed, based on an earlier single nozzle model described by Renaudo et al. (2022). The extended model, which also includes droplets dispersion in the vertical direction, was successfully calibrated and then validated with field data from sources that covers different process conditions. In fact, the calculated spray drift values showed good agreement with reported measurements in a wide range of distances in the downwind direction. For the studied cases, the eddy diffusivity was found to be a function of the relative humidity. In the absence of dispersion-related data, the fitted equation can be used to fully predict spray drift from horizontal boom sprayers. The results indicated that, as the downwind distance increases, more nozzles contribute to the deposited flowrate and therefore accounting for them is necessary for a good representation of the spray drift. The model demonstrated to have low computational costs (time and resources) being then suitable to be used on board sprayer computers and web servers.

1. Introduction

Agrochemicals play an important role in modern agriculture to meet food security by increasing field crops productivity and quality (Pretty, 2008; Pretty & Bharucha, 2014). For ground applications, agrochemicals are normally applied by spraying solutions, emulsions or suspensions through nozzles mounted on a boom. During spraying, a fraction of the atomized liquid may not reach the target area, being transported by wind to greater distances. The process by which atomized droplets are deposited off-target is known as spray drift, and it is a major concern because it affects human health and the environment (Lebeau et al., 2011).

In horizontal boom sprayers, the spray nozzles are distributed on the boom evenly spaced. Long booms allow the application of agrochemicals over a large work area, reducing the time required for spraying (Nuyttens, 2007). Because of this, droplets deposited at a given distance can be originated from any of the boom nozzles located upstream. The boom and components of the sprayer system can block the airflow below the boom (Teske et al., 2011). Although, the nozzle characteristics influence the spray drift greater than the boom structure itself (Murphy et al., 2000). Besides the nozzles type, number and location in the boom, the spray operating conditions and environmental factors greatly affect the atomized droplet size distribution, the droplets movement behavior and consequently the spray drift (Onorato & Tesouro, 2006).

* Corresponding author. Departamento de Ingeniería Química, Universidad Nacional del Sur (UNS), Argentina.
E-mail address: carenaudo@plapiqui.edu.ar (C.A. Renaudo).

Note: Low-resolution images were used to create this PDF. The original images will be used in the final composition.

Many efforts were performed to improve the spray drift prediction in ground applications to avoid time-consuming and expensive measurements (Butler Ellis & Miller, 2010). The droplet tracking models (lagrangian approach) is particularly appropriate to represent the droplets behavior near the nozzle. As a disadvantage, the execution time increases as the number of trajectories and distance to be modeled increase. The turbulent dispersion phenomenon should be coupled to Lagrangian models for good spray drift predictions over long downwind distances. In fact, Holterman et al. (1997) developed the IDEFICS model that uses the random-walk approach to represent the turbulence. To correctly predict spray drift, this model included evaporation and air drag phenomena, as well as spatial profiles of the wind speed over and within the crop. Based on work of Miller and Hadfield (1989), Buttler Butler Ellis and Miller (2010) also developed a spray drift model based on a Lagrangian approach including a random component to describe the turbulence. The use of the random-walk approach increases the number of trajectories required to be modeled and consequently the computational cost.

Bilanin et al. (1989) uses a Lagrangian approach, for aerial applications, to estimate droplets trajectories to calculate deposition in the target area. Their model was called AGricultural DISPersal (AGDISP) model, and it was updated over time. Teske et al. (2004) included a gaussian steady state model to AGDISP for aerial application. Later, Teske et al. (2009) developed a boom ground spray drift predictor based on AGDISP, however the model is not fully described.

The gaussian plume modeling is an alternative approach to account for the turbulent dispersion. For this representation, a statistical gaussian distribution of the droplets concentration around their trajectories is considered. The main advantage of this approach is the computational efficiency, particularly when long distances downwind need to be modeled (Butler Ellis & Miller, 2010). Lebeau et al. (2011) developed the RTDrift software, which uses a phenomenological Gaussian plume model to estimate spray drift for a boom sprayer. They used a force balance to estimate the mean trajectory of droplets after solving the motion equations. The authors concluded that, after comparing the model results with experimental measurements, the model produces realistic maps of drift deposits for various wind conditions. Even though the model is suitable to represent field data, the authors do not explore the effect of the nozzles on spray drift and the equations that relates it with the boom properties (number of nozzles and spacing) are not explicitly given.

Renaudo et al. (2022) presented a coupled atomization-spray drift model suitable for different types of nozzles. The authors, for a single nozzle, developed a simulation tool using input data that are easily accessible by applicators (spray pressure, nozzle model and nominal flowrate, spray angle, sprayer speed and environmental conditions). The authors formulated the droplets motion equations based on a modified Lagrangian approach. Using a bivariate continuous function that describes the initial conditions of the spray (i.e., the droplet size distribution and the spray distribution pattern), the spray drift can be calculated analytically. Avoiding the equations discretization, the model execution time is reduced overcoming one of the main disadvantages attributed to the conventional lagrangian model.

In this contribution, the single nozzle model described by Renaudo et al. (2022) is extended to predict the spray drift from horizontal boom sprayers by considering the effect of the turbulent dispersion and boom nozzles number and spacing on the spray drift. Therefore, this model takes the advantages of the model of Renaudo et al. (2022) in terms of computational efficiency by describing distributions in a continuous rather than discrete manner. In the paper, the equations that allow to calculate the spray drift for a horizontal boom sprayer as a function of variables known by the applicator are presented explicitly. In relation to the dispersion coefficient, this parameter was studied, and a fitted function dependent of relative humidity is provided. This model, which is calibrated and validated against different reported field data, seeks to be suitable for use sprayer on-board even with very low resource computers or cloud server. Summarizing, the proposed modeling approach provides a simple, accurate and computationally efficient tool to predict the droplets fate from horizontal boom sprayers.

2. Mathematical model

The presented model extends the work of Renaudo et al. (2022) to predict the spray drift to horizontal boom sprayers by considering multiple nozzles and the dispersion phenomena. It is formulated based on the following assumptions.

   i. The atomized droplet size distribution (DSD) is represented by an Upper Limit Lognormal (ULLN) function (Hong et al., 2018), whose parameters are obtained from characteristics diameters of experimental DSDs.
   ii. Droplets leave the nozzle in different directions. Therefore, there is a distribution of initial trajectories for the atomized droplets. This distribution is represented by means of a Gaussian function (Mawer & Miller, 1989).
  iii. The initial trajectories of the droplets are independent of their initial sizes.
   iv. Droplet movement is influenced by the wind, but the wind is not influenced by the particles (i.e., no air entrainment is considered).
   v. Sprays from adjacent nozzles are non-interacting.
   vi. Atomization and deposition of droplets occur in steady state.
  vii. Droplets are spherical and have constant viscosity and density.
 viii. The wind velocity is a function of the vertical coordinate (z). The droplets, during their flight, horizontally move at the wind velocity. Therefore, the droplets undergo different velocities as function of their vertical position.
   ix. In the vertical direction, the velocity of a droplet of a given size is equal to its terminal velocity (v_T) (Lebeau et al., 2011; Løfstrøm et al., 2013). Although the initial droplet velocity is higher than the terminal one at the nozzle exit, small droplets quickly reach the terminal velocity, while large droplets would be deposited in the same place regardless of whether the initial or terminal velocity is considered.

x. All the droplets with given initial size and angle have the same flight time, evaporation loss and terminal velocity (Stainier et al., 2006; Tan, 2014).

xi. Droplets are deposited as soon as they reach the soil surface.

xii. The evaporation rate of droplets is that of pure water (Teske et al., 2016). That is, the active ingredient of droplets is present in low concentration and has lower volatility than water (Finch et al., 2014).

xiii. Turbulent dispersion in the vertical direction is represented by a Gaussian distribution (Bilanin, 1989; Jacobson, 2005). In the x-direction, dispersion is neglected because transport by wind is considered higher than the turbulent dispersion effect (Bozon et al., 2009; De Visscher, 2013; Tan, 2014).

xiv. The sprayer moves with forward speed constant and perpendicular to the wind velocity direction. The impact of the sprayer forward speed on the spray drift is neglected.

2.1. Atomized droplet distribution

Based in assumption iii, the population of droplets atomized by each nozzle is represented by the following continuous bivariate function (Renaudo, 2020; Renaudo et al., 2022):

$$f_{dx_0}\left(d_0, x_0\right) = f_d\left(d_0\right) f_{x_0}\left(x_0\right) \tag{1}$$

$f_{dx_0}\left(d_0, x_0\right)$ provides the probability of a droplet (generated by a single nozzle) to have a determined initial size d_0 and deposition distance x_0.

In Equation (1), $f_d\left(d_0\right)$ is the droplet size distribution (DSD). According to assumption i, the volume density function (Allen 2013) of the droplets atomized by each nozzle is given by the upper-limit log-normal (ULLN) function:

$$f_d\left(d_0\right) = \begin{cases} \dfrac{1}{\sqrt{2\pi}\ \ln\ \sigma_{ul}}\dfrac{d_{\max}}{d_0(d_{\max}-d_0)}e^{-\frac{1}{2}\left[\frac{\ln(a_{ul}d_0)-\ln(d_{\max}-d_0)}{\ln\ \sigma_{ul}}\right]^2} & d < d_{\max} \\ 0 & d \geq d_{\max} \end{cases} \tag{2}$$

where a_{ul} and σ_{ul} represent the mean and standard deviation of the ULLN function, while $d_{\max}$ is the maximum droplet diameter of the DSD. d_0 is the independent variable of the function and corresponds to the atomized droplet diameter. The parameters of the ULLN function are related to representative diameters (D_{V10}, D_{V50} and D_{V90}) of the volumetric atomized droplet size distribitution as follows (Mugele and Evans, 1951):

$$d_{\max} = D_{V50}\left(\frac{D_{V50}\left(D_{V10}+D_{V90}\right) - 2D_{V10}D_{V90}}{\left(D_{V50}\right)^2 - D_{V10}D_{V90}}\right) \tag{3}$$

$$\sigma_{ul} = \left[\left(\frac{d_{\max}-D_{V50}}{d_{\max}-D_{V90}}\right)\frac{D_{V90}}{D_{V50}}\right]^{0.7794} \tag{4}$$

$$a_{ul} = \frac{d_{\max}-D_{V50}}{D_{V50}} \tag{5}$$

In Equation (1), $f_{x_0}\left(x_0\right)$ represents the spray distribution pattern (SDP), which describes the spatial distribution of droplets deposited on the ground under conditions of zero wind speed (Renaudo et al., 2022). Based on Mawer and Miller (1989), $f_{x_0}\left(x_0\right)$ is represented by means of a Gaussian distribution as a function of the deposition distance x_0:

$$f_{x_0}\left(x_0\right) = \frac{1}{\sqrt{2\pi}\sigma_s}\exp\left[-\frac{1}{2}\left(\frac{x_0}{\sigma_s}\right)^2\right] \tag{6}$$

where σ_s is set so that the following equations are satisfied (Mawer & Miller, 1989; Leunda et al., 1990):

$$f_{x_0}\left(\frac{H}{\tan\ \theta}\right) = f_{x_0}\left(-\frac{H}{\tan\ \theta}\right) = 1e^{-6} \tag{7}$$

where θ represents the spray angle and H the boom height.

By replacing equations (2) and (6) in 1, it is obtained:

$$f_{dx_0}\left(d_0, x_0\right) = \begin{cases} \dfrac{1}{2\pi\ \sigma_s\ \ln\ \sigma_{ul}}\dfrac{d_{\max}}{d_0(d_{\max}-d_0)}e^{-\frac{1}{2}\left[\frac{\ln(a_{ul}d_0)-\ln(d_{\max}-d_0)}{\ln\ \sigma_{ul}}\right]^2-\frac{1}{2}\left(\frac{x_0}{\sigma_s}\right)^2} & d_0 < d_{\max} \\ 0 & d_0 \geq d_{\max} \end{cases} \tag{8}$$

2.2. Droplets Lagrangian behavior

2.2.1. Droplet diameter change by evaporation

During the evaporation of a droplet in flight, it is commonly assumed that a spherical droplet with diameter d evaporates at a rate proportional to its exposed surface area (Lebeau et al., 2011; Onorato & Tesouro, 2006). Under this assumption, the diameter of the droplet varies linearly with time. On the other hand, Amsden (1962) demonstrated that the lifetime of a droplet is kd_0^2, where k depends on the dry and wet bulb temperatures of the ambient air. Therefore, the decrease in droplet diameter by evaporation can be modeled as a function of time using the following equation:

$$d = \begin{cases} d_0 \left(1 - \frac{t}{kd_0^2}\right) & t < kd_0^2 \\ 0 & t \geq kd_0^2 \end{cases} \tag{9}$$

where t is the time and k is given by:

$$k = \frac{10^{12}}{\beta \left(T - T_{wb}\right)} \tag{10}$$

T and T_{wb} correspond to the dry and wet bulb temperatures, respectively. The constant β is equal to $80 \ 10^{12} \ m^2/s \ °C$ (Lebeau et al., 2011). T_{wb} is calculated as a function of T and the relative humidity RH using the following empirical correlation of Stull (2011).

2.2.2. Vertical distance traveled by a droplet ($\bar{z}$)

The vertical distance $\bar{z}$ traveled by a droplet varies according to its terminal velocity v_T (assumption ix). Assuming Stokes regime (Zannetti, 2013):

$$\frac{d\bar{z}}{dt} = v_T = \frac{\Delta\rho g d^2}{18\mu_g} \tag{11}$$

where $\Delta\rho$ is the difference between the density of the droplet and that of the air, μ_g is the air viscosity, g is the gravity acceleration and d represents the diameter of the droplet in flight.

From equations (9) and (11), the following equation is obtained:

$$\bar{z} = -\frac{kd_0\Delta\rho g}{54\mu_g}\left(d^3 - d_0^3\right) \tag{12}$$

Equation (12) relates the vertical distance traveled by a droplet of initial size d_0 when its diameter decreases to d.

2.2.3. Minimum initial diameter of deposited droplets ($d_{\min}$)

From Equation (12) it is possible to calculate the initial droplet diameter that completely evaporates when reaches the ground. By considering $d = 0$ and $\bar{z} = H$ in equation (12), $d_{\min}$ is calculated as follows:

$$d_{\min} = \left(\frac{54\mu_g H}{k\Delta\rho g}\right)^{\frac{1}{4}} \tag{13}$$

2.2.4. Droplet critical diameter (d_{crit})

This diameter refers to the maximum initial diameter d_0 that an atomized droplet must have to be affected during its trajectory by the wind before being deposited. d_{crit} is calculated as:

$$d_{crit} = \left[\frac{54\mu_g H}{k\Delta\rho g}\frac{1}{1 - \left(1 - \frac{\rho_d}{18k\mu_g}\right)^3}\right]^{1/4} \tag{14}$$

The derivation of Equation (14) is provided in Appendix A.

2.2.5. Effective wind speed

The wind velocity profile is given by the following equation (Jacobson, 2005; Richards & Norris, 2011; Tan, 2014):

$$U = U_0 \frac{\ln\left(\frac{(H-z)+\varepsilon}{\varepsilon}\right)}{\ln\left(\frac{H+\varepsilon}{\varepsilon}\right)} \tag{15}$$

where z is the vertical spatial coordinate, U_0 is the wind speed at the nozzle height ($z = 0$) and ε is the surface roughness. For relatively flat terrains, such as those corresponding to fallow fields, ε is considered equal to 0.09 (Lebeau et al., 2011; Tieleman, 2003).

According to assumption *viii*, the droplets horizontally move at the wind velocity. Therefore, the droplets undergo different velocities as function of their vertical position (which is related to its initial size and flight time, as it will be shown in Equation (19)). In order to have an effective horizontal velocity of the droplets population, Equation (15) is averaged with respect to the droplet flying time and initial diameter:

$$\bar{U} = \frac{\int_{d_{\min}}^{d_{\max}} \int_{t_0}^{t_{dep}} U\left(z = \bar{z}t, d_0\right) f_d\left(d_0\right)\ dt\ dd_0}{\int_{d_{\min}}^{d_{\max}} \int_{0}^{t_{dep}} f_d\left(d_0\right)\ dt\ dd_0} \tag{16}$$

According to the t_{resp} definition (see Appendix A), if time is lower than the response time the droplet is not affected by the drag ($U = 0$). Regarding droplets diameter, droplets with initial diameters higher than d_{crit} will not be affected by the wind ($U = 0$). Taking into account these considerations, Equation (16) can be rewritten as:

$$\bar{U} = \frac{\int_{d_{\min}}^{d_{crit}} \int_{t_{resp}}^{t_{dep}} U f_d\left(d_0\right)\ dt\ dd_0}{\int_{d_{\min}}^{d_{\max}} \int_{0}^{t_{dep}} f_d\left(d_0\right)\ dt\ dd_0} \tag{17}$$

In this way, Equation (17) provides the single value for the droplets velocity in x-direction, which weights the wind speed by the size distribution and flight time of droplets that are influenced by wind speed. This strategy avoids the use of different speeds for each droplet size and flight time by using a constant value of speed that is physically representative for droplets moving downwind. Equation (17) can be solved numerically for any wind velocity profile and atomized DSD.

2.2.6. Horizontal distance traveled by a droplet

Due to assumption viii, the horizontal distance traveled by a droplet is quantified by the following equation:

$$x = x_0 + \bar{U}t \tag{18}$$

In Equation (18), x has two contributions: the first term that depends only on the initial trajectory of the droplet and a second one that represents the distance traveled due to the wind.

In Appendix A, the droplet flight time as a function of the traveled vertical distance $\bar{z}$ is calculated as:

$$t = kd_0^2\left[1 - \left(1 - \frac{54\mu_g \bar{z}}{kd_0^4 \Delta\rho g}\right)^{\frac{1}{3}}\right] \tag{19}$$

Replacing Equation (19) in 18, the following expression is obtained:

$$x = x_0 + \bar{U}kd_0^2\left[1 - \left(1 - \frac{54\mu_g \bar{z}}{kd_0^4 \Delta\rho g}\right)^{\frac{1}{3}}\right] \tag{20}$$

Equation (20) allows to calculate the horizontal distance traveled by each droplet as a function of the droplets initial conditions (d_0, x_0) and the traveled vertical distance $\bar{z}$.

2.3. Dispersion of droplets in flight

If there is no turbulent dispersion, all droplets with the same initial conditions (d_0, x_0) have the same trajectory (defined by equations (12) and (20)) and the model developed by Renaudo et al. (2022) for one nozzle can be used. However, due to the dispersion phenomenon, droplets tend to deviate from this path in such a way that there is a density of droplets around their trajectory. Therefore, for each class of droplets with initial conditions (d_0, x_0) in the presence of turbulent dispersion, the trajectory obtained with the model without dispersion is the *mean* trajectory of this droplet class.

In dispersion models, concentration of droplets in flight in the vertical direction is commonly represented by a Gaussian distribution (Bilanin, 1989; Jacobson, 2005; Lebeau et al., 2011):

$$f_{disp}(\Delta z) = \frac{1}{\sigma_z \sqrt{2\pi}} e^{-\frac{\Delta z^2}{2\sigma_z^2}} \tag{21}$$

As it is schematized in Fig. 1, f_{disp} is a density function that represents the droplets distribution in the vertical axis, σ_z is the standard deviation of the Gaussian distribution and Δz is $z - \bar{z}$ (i.e., the vertical distance from the mean trajectory). Equation (21) can be rewritten to provide the density function of droplets that reach the ground as follows:

$$f_{disp}(\bar{z}) = \frac{1}{\sigma_z \sqrt{2\pi}} e^{-\frac{(H-\bar{z})^2}{2\sigma_z^2}} \tag{22}$$

In Equation (22), a change of variables is required to express the dispersion function in terms of x:

$$f_{disp}(x) = \frac{d\bar{z}}{dx} \frac{1}{\sigma_z \sqrt{2\pi}} e^{-\frac{(H-\bar{z})^2}{2\sigma_z^2}} \tag{23}$$

According to assumption xiii, dispersion in the wind direction is not considered. For this reason, the movement of droplets in this direction is still represented by Equation (20). According to assumption viii-xi, it is verified:

$$\frac{d\bar{z}}{dx} = \frac{\frac{d\bar{z}}{dt}}{\frac{dx}{dt}} = \frac{v_T}{\bar{U}} \tag{24}$$

where v_T is calculated by Equation (11).

Replacing Equation (24) in 23, f_{disp} becomes:

$$f_{disp}(x) = \frac{v_T}{\bar{U}} \frac{1}{\sigma_z \sqrt{2\pi}} e^{-\frac{(H-\bar{z})^2}{2\sigma_z^2}} \tag{25}$$

In addition $\bar{z}$ in Equation (25), by means of Equation (20), can be related to the distance x as follows:

$$\bar{z} = \frac{d_0^4 \Delta \rho g}{54 \mu_g} \left[1 - \left(1 - \frac{x - x_0}{\bar{U} k d_0^2} \right)^3 \right] \tag{26}$$

The dispersion coefficient σ_z is a function of atmospheric turbulence, surface roughness, average wind speed and the distance traveled by the droplet (Tan, 2014). In general, σ_z is expressed as (Liu et al., 2018; Seinfeld & Pandis, 2016):

$$\sigma_z = C_1 (x - x_0)^{C_2} \tag{27}$$

where

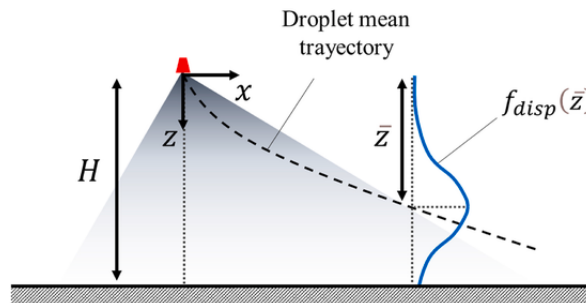$$C_1 = \sqrt{\frac{2D_Z}{\bar{U}}} \tag{28}$$

Fig. 1. Mean trajectory of atomized drops and dispersion function.

In Equation (28), D_Z is the eddy diffusivity in the z coordinate. In the literature, different values are suggested for D_Z and C_2, which are dependent on environmental conditions. These values are often used in dispersion models ranging from tens of meters to hundreds of kilometers (e.g., Lebeau et al., 2011; Liu et al., 2018; Seinfeld & Pandis, 2016; Venkatram, 1996).

2.4. Distribution function of deposited droplets

2.4.1. Single nozzle

For a nozzle, the distribution function of active ingredient deposited at distance x for droplets with initial condition (d_0, x_0), is obtained by multiplying the density functions given by equations (8) and (25):

$$f_{d,x_0,x} = f_{d_0}(d_0)f_{x_0}(x_0)\frac{v_T}{\overline{U}}\frac{1}{\sigma_z\sqrt{2\pi}}e^{-\frac{(H-\overline{z})^2}{2\sigma_z^2}} \tag{29}$$

As already mentioned, Equation (26) relates $\overline{z}$ to d_0, x_0 and x. Integrating for all d_0 and x_0, the density function of active ingredients is obtained for the entire population of atomized droplets:

$$f_x(x) = \int_{-H/\tan\theta}^{H/\tan\theta}\int_{d_{\min}}^{d_{\max}}f_{d_0}(d_0)f_{x_0}(x_0)\frac{v_T}{\overline{U}}\frac{1}{\sigma_z\sqrt{2\pi}}e^{-\frac{(H-\overline{z})^2}{2\sigma_z^2}}dd_0 dx_0 \tag{30}$$

2.4.2. Multiple nozzles

The volumetric flowrate atomized by each nozzle is calculated as (Post et al., 2017):

$$Q = C_d A_n\sqrt{\frac{2P}{\rho_d}} \tag{31}$$

where C_d is the discharge coefficient, A_n is the nozzle orifice area, P is the atomization pressure and ρ_d is the droplets density. For a boom with N nozzles, the total liquid flowrate atomized (Q^{boom}) is calculated as:

$$Q^{boom} = NQ \tag{32}$$

To determine the deposition function of active ingredients, the coordinate system origin is set at the end nozzle of the boom, as indicated in Fig. 2. Assuming that the nozzles are equal and considering assumption iv and v (i.e., one-way coupling approach), the distribution function of active ingredients deposited for the i-th nozzle (f_x^i) is represented as:

$$f_x^i(x) = f_x(x + (i-1)s) \tag{33}$$

where s is the nozzles spacing.

The distribution function of active ingredients deposited for the complete boom (f_x^{boom}) is obtained by adding the contributions of all the nozzles:

$$f_x^{boom}(x) = \sum_{i=1}^{N}f_x^i(x) = \sum_{i=1}^{N}f_x(x + (i-1)s) \tag{34}$$

Spray drift is defined as the ratio between the volume of active substance deposited per unit area and the applied dosage. It can be calculated from $f_x^{boom}(x)$ as follows:

$$Y(x) = \frac{V_{dep}/A}{F} = \frac{Q}{v_A F}f_x^{boom}(x) = sf_x^{boom}(x) \tag{35}$$
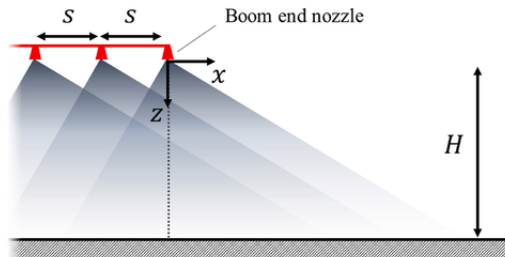

Fig. 2. Schematic diagram of a boom with multiple nozzles.

where V_{dep} is the volume deposited in the area A, F is the atomized dose (liquid volume per unit area) and v_A is the sprayer speed. Then, to finally evaluate the spray drift at a given downwind distance for a horizontal boom, the environmental conditions, nozzle type, nominal flowrate, spray angle and operating pressure have to be defined.

The calculation steps are schematically illustrated in Fig. 3. To define a case, it is necessary to provide the atomized DSD and SDP (experimental data or ULLN parameters and σ_s), the boom height (H), the weather conditions (wind velocity, temperature and relative humidity) and the sprayer information (forward speed, number of nozzles and spacing). The effective wind speed of the atomized cloud (Equation (17)) is calculated based on the DSD, wind velocity profile and the boom height. The effective wind speed combined with the other input variables are used in module 1 to predict the droplet deposition at any given downwind distance generated by a single nozzle. The model can be executed including or not the dispersion phenomenon. The deposition calculated in the module 1 (Equation (30)) combined with the sprayer information is used in the module 2 to predict the spray drift at a given downwind distance (equations (34) and (35)). This information can be postprocessed to calculate desired key sprayer performance indicators (KSPIs).

The model (defined by Equations ((8)–(14) and (17) and (30) and (34) and (35)) was executed in a windows 10 desktop PC with a Intel Core i7 4790S and 8 Gb of RAM using the Python 3.10 programming language and the *NumPy* module (Numpy, 2023). The integrals of Equation (30) were solved using the trapezoidal rule (*trapz* function of *Numpy*) with an arithmetic discretization of 10 elements for x_0 (between $-H/\tan\theta$ and $H/\tan\theta$) and a geometric discretization of 30 elements for d_0 (between $d_{\min}$ and $d_{\max}$). *timeit* module was used analyze the average execution time of the different steps of the model (Python, 2023). As expected, the step more computational-time consuming corresponds to module 1 (0.0018 s for results at a given distance). The total execution time is proportional to the number of nozzles and distances whose spray drift is wanted to be computed. Equation (17) is solved only once for each simulation case, (0.00167s of execution time). The model was also implemented in PHP 8 (no external libraries used) and executed in a google cloud virtual machine (f1-micro virtual processor, 0.6 Gb of RAM). In this case, the execution time of the module 1 was 0.003 s.

3. Results

3.1. Multiple nozzle boom spray model: calibration and validation

Nuyttens (2007) measured the spray drift in field conditions applying the procedure established by ISO 22866. Within the reported data by Nuyttens, 9 and 15 cases were selected to respectively calibrate and validate the model presented in this contribution. Since for each case, Nuyttens reported the spray drift at 8 distances, then the selected cases provide a total of 192 spray drift values. For the selected tests it is verify that: the sprayer forward and wind directions were approximately perpendicular, and the wind speed was higher than 1.5 m/s. This last condition is required to fulfill assumption xiii, i.e. convective effects are greater than the dispersive ones in the wind direction (Tepper, 2012). A detailed description of the procedure used in the field test was reported by Nuyttens (2007).

Fig. 4a and 4b summarize the environmental conditions (wind speed, temperature and relative humidity) of the tests considered for calibration and validation, respectively. Due to the fluctuations of the meteorological conditions during each test, the reported average values for U_0, T and RH were considered (Nuyttens, 2007). For all cases, the nozzles separation was 0.5 m and the horizontal boom height varied between 0.3 and 0.75 m. Different nozzles and spray pressures were used for each test, generating D_{V10}, D_{V50} and D_{V90} values of the atomized aerosol in the ranges of 90–290 μm, 240–580 μm and 370–1000 μm, respectively. The experimental
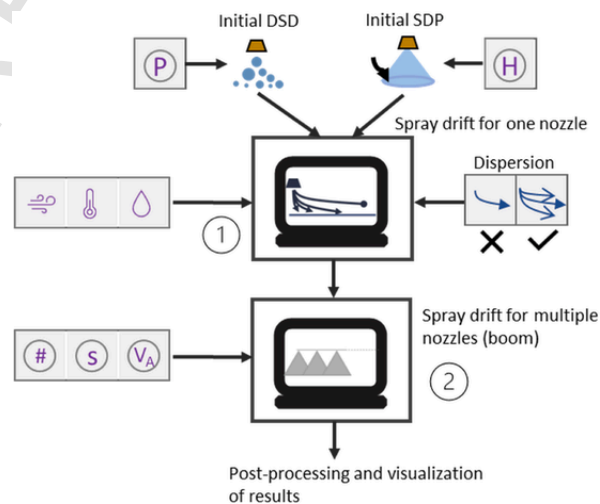

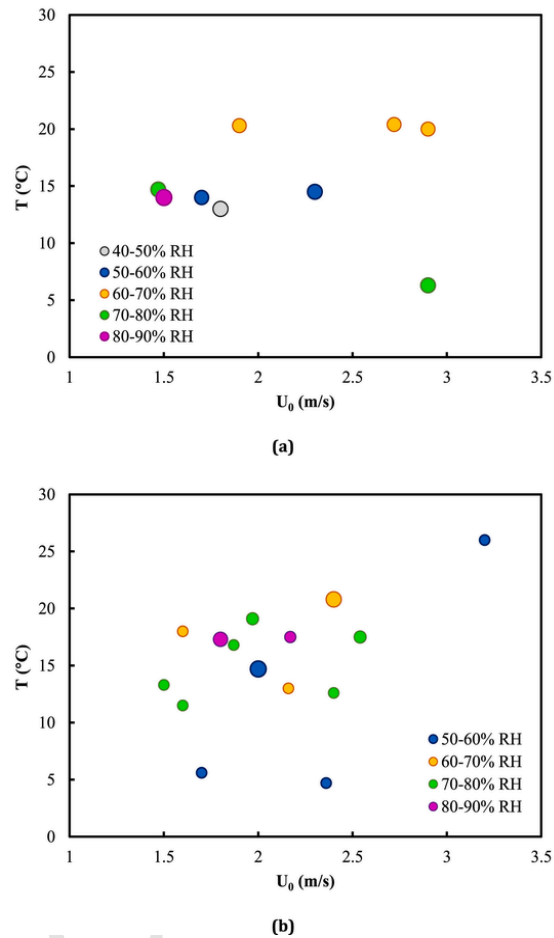**Fig. 3.** Calculation steps to provide droplets deposition information.

Fig. 4. Wind speed, temperature and relative humidity of the experimental tests carried out by Nuyttens (2007) and used for a) calibration and b) validation of the dispersion model. The relative size of the circles is an indicator of the D_{V50} of the atomized DSD.

DSDs reported by Nuyttens (2007) were measured in an insulated controlled climate room using an Aerometrics Phase Doppler Particle Analyzer (PDPA) (TSI, Minneapolis) about 50 cm from the nozzle exit.

For each of the 9 tests selected for calibration (Fig. 4a), the values of C_1 and C_2 were obtained by minimizing the mean square error between the experimental and calculated spray drift values. C_2 remained almost constant for all the tests. For each case, one D_Z value was calculated from the corresponding C_1 (see Equation (28)).

The dispersion coefficients and eddy diffusivity of atmospheric air are influenced by several factors. For example, Briggs et al. (1973), related the dispersion coefficients to atmospheric stability. In turn, atmospheric stability was found to be associated with a large number of climatic variables, such as: wind speed (Pasquill, 1961), wind direction (Slade, 1968), air temperature and thermal gradient (Golder, 1972), irradiation (Turner, 1964), relative humidity (Brugge, 1996; Iturbide-Sanchez et al., 2016).

In this work the calculated D_Z values were, separately, correlated with wind velocities at two heights, mean velocity, wind direction, temperature, relative humidity, thermal gradient and atmospheric stability (data available from Nuyttens, 2007). From this study, it was found that the calculated D_Z was well correlated as a function of the relative humidity ($R^2 = 0.98$). This result is in good agreement with Giri et al. (2008) and Kayes et al. (2019), who reported that the relative humidity is one of the most important meteorological parameters influencing the behavior of air pollutants. Fig. 5 shows D_Z (fitted parameter) as a function of RH. It can be observed that the experimental data can be reproduced adequately (dotted line) by means of the following equations:

$$D_Z = 0.0038 \left(\frac{RH}{100} \right)^{-10/3} \tag{36}$$

$$C_2 = 0.85 \tag{37}$$

In equation (36), the value of RH is expressed as percentage and the unit of D_Z is m^2/s. The C_1 and C_2 values are within the range of the ones reported in the literature (0.017–0.4 and 0.5–1.38 and for C_1 and C_2, respectively, according to Seinfeld & Pandis, 2016).
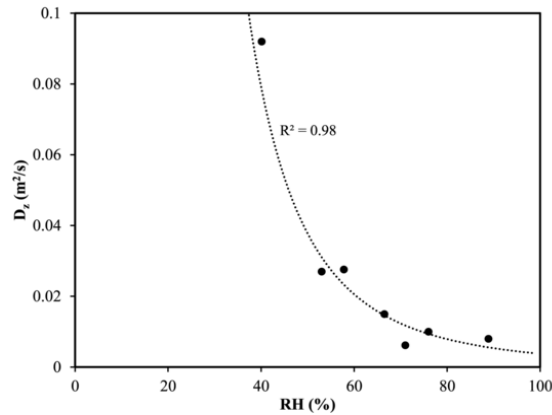
Fig. 5. Fitted D_Z values as a function of the relative humidity. The dotted line corresponds to Equation 39.

As already mentioned, 15 tests reported by Nuyttens (2007) were used to validate the fitted model. In Fig. 6 experimental and predicted spray drift values are compared. The results are presented in different colors to indicate the measurement distance, and different shapes to indicate if the data was used for model calibration or validation purposes (triangles: calibration, squares: validation). Løfstrøm et al. (2013), when comparing experimental and predicted values of spray drift reported that 82% of the calculated drift (Y) values were in the range of ($Y/4$; $4Y$) and concluded that the fit was satisfactory. For the model presented in this manuscript, 87% of the data used for validation fulfill the Løfstrøm's criterium. Besides, the correlation coefficient between the experimental and calculated data was $R^2 = 0.86$ for the data used for validation (for distances between 0.5 and 10 m). For these reasons, a good correspondence between the simulated and experimental values was observed for distances lower than 10 m. For longer distances the model underestimates the spray drift, however, at those distances the spray drift is very low.

3.2. Further model validation

To investigate whether the fitted model using experimental data from Nuyttens (2007) can be applied to measurements by other authors, the model was validated against data from van de Zande et al. (2014). These authors carried out 6 spraying tests in the field following the ISO 22866 standard and reported spray drift as a function of distance. The nozzles used in each experiment were different, for the assay here called V1 a standard flat-fan nozzle was used, while for the other cases drift-reducing nozzles were employed (assay V2: pre-orifice nozzle, assays V3–V6: air-induction nozzles). Table 1 presents D_{V10}, D_{V50} and D_{V90} of the atomized droplet distribution for each test. Regarding the DSDs measurements, the reported data correspond to values obtained through the PDPA technique about 50 cm from the nozzle exit (van de Zande et al., 2014). In particular, for cases V5 and V6 the DSDs presented D_{V10} and D_{V50} values outside of the data range reported by Nuyttens (2007), which provides more variability to test the model. The spraying
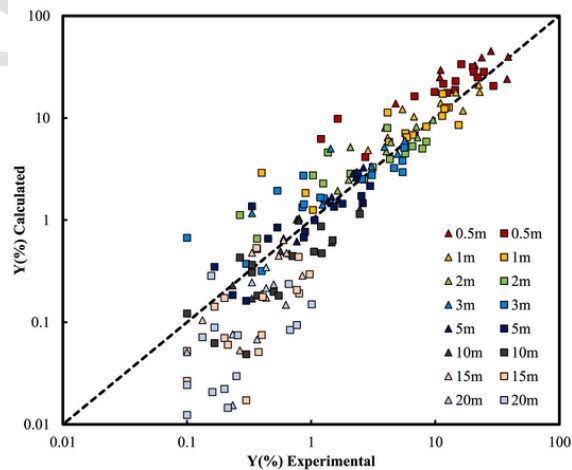

Fig. 6. Comparison between experimental results of Nuyttens (2007) and those calculated by the fitted mathematical model. Triangles: data used for calibration, squares: data employed for validation.

Table 1

D_{V50} of the atomized spray for each test of van de Zande et al. (2014).

Assay	D_{V10} (µm)	D_{V50} (µm)	D_{V90} (µm)
V1	140	274	434
V2	168	322	507
V3	251	485	794
V4	256	573	913
V5	348	646	967
V6	332	648	982

pressure was 3 and 1 bar for the cases V1–V4 and V5–V6, respectively. The average wind speed at the boom height was $\bar{U} = 1.5$ m/s, the temperature 9 °C, the relative humidity 80% and the wind direction had a 20° of deviation from perpendicular to the sprayer advance direction. According to Smith et al. (2000), the deposited distance was corrected ($x_{dep}^{sim} = x_{dep}^{exp} \cos(20^o)$) to consider the wind direction deviation. The boom height and the separation between nozzles were both 0.5 m.

In Fig. 7 the calculated and experimental spray drifts are compared for tests V1 and V2 as a function of the deposition distance. For better visualization, the results are presented using both linear and logarithmic scales. To demonstrate that the dispersion phenomenon impacts the model results, Fig. 7 also includes the simulations without considering dispersion ($\sigma_z \rightarrow 0$). As expected, for all cases, spray drift increases when dispersion is considered. This is because turbulence causes the droplets to stay in flight longer and, consequently, to settle at greater distances. Although the spray drift as a function of distance is described as a decreasing function by both models, the fitted model including dispersion is clearly superior. Even so, it is observed that, for distances less than 2 m, the model without dispersion well describes the spray drift. This is important because, if spray drift is evaluated at distances less than 2 m, the presented model without any adjustable parameter ($\sigma_z = 0$) would be enough accurately for prediction purposes.

For V3–V6 tests, Fig. 8 presents the calculated axial drift profiles (with and without dispersion) using a linear scale for the y-axis (spray drift). For the V5 assay, both models provide similar results up to 3 m, but underestimate the very low drift values found for longer distances. For the V3, V4 and V6 test, the model with dispersion adequately predicts the experimental data for the entire range of distances, while the model without dispersion gives adequately predictions up to a distance of around 2 m.
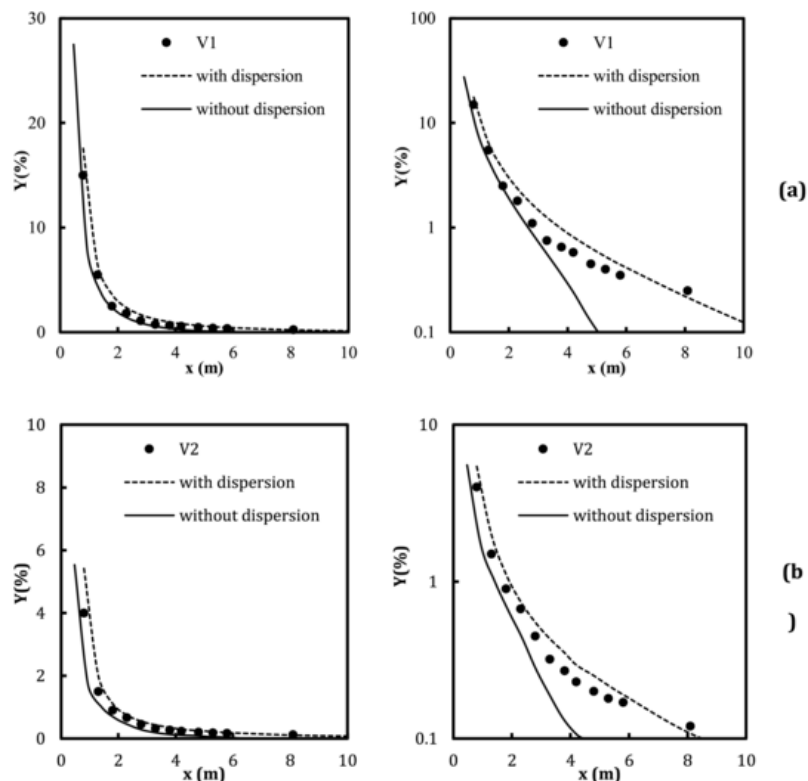

Fig. 7. Comparison between experimental results of van de Zande (2014) and those predicted by the model with dispersion (dashed line) and without dispersion (continuous line) for cases a) V1 and b) V2. Both linear and logarithmic scales are used to display Y.
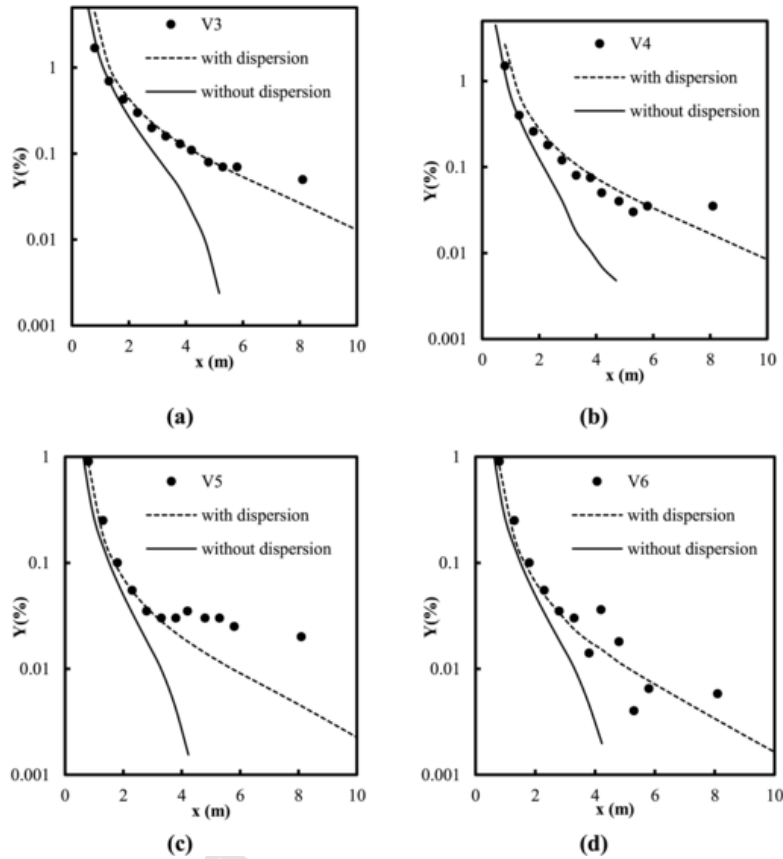
Fig. 8. Comparison between experimental results of van de Zande (2014) and those predicted by the model with dispersion (dashed line) and without dispersion (continuous line) for cases a) V3, b) V4, c) V5 and d) V6.

The calibrated model fulfills the Løfstrøm's criterium for 80% of the measurements reported by van de Zande et al. (2014). Besides, the correlation coefficient between the experimental and calculated data, shown in Figs. 7 and 8, was $R^2 = 0.95$ (for distances between 0.5 and 10 m).

3.3. Single nozzle vs multiple nozzles

To analyze the influence of the nozzle number on droplets deposition, simulations were performed varying the nozzle number from $N = 1$ (i.e., single nozzle) to $N = 54$. The simulations are based on a selected case of the ones reported by Nuyttens (2007), that was used for the model validation. The model input variables are presented in Table 2. Fig. 9 compares experimental spray drift results (including error bars) with the simulated values for $N = 1$ (i.e., single nozzle) and $N = 54$ (i.e., complete boom). The inclusion of the multiple nozzles in the model allows to predict the experimental spray drift satisfactorily. As expected, the presence of the multiple nozzles produces an increase in the spray drift values as a consequence of the contribution of all the nozzles; mathematically expressed as the summation of deposition functions (Equation (34)). For this case, at 1, 3 and 5 m, the boom spray drifts are 2, 5 and 7 times higher than the ones predicted by using one nozzle, respectively.

Table 2
Common process variables values for results of Fig. 9.

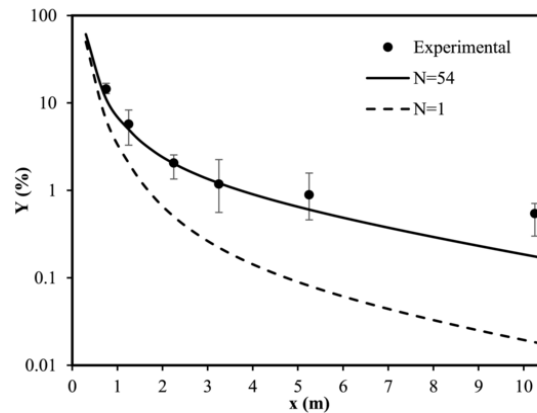| Variable	Value
T (°C)	18
RH (%)	64
U_0 (m/s)	1.7
D_{V10} (μm)	144
D_{V50} (μm)	273.6
D_{V90} (μm)	421.9
H (m)	0.5
s (m)	0.5

Fig. 9. Comparison between experimental spray drift and predictions of the model for $N = 1$ and $N = 54$.

Fig. 10 shows the fraction that each nozzle contributes to the total deposited flowrate. On the x-axis of Fig. 10, nozzle 1 corresponds to the one located at x = 0 m (i.e., the position of the last nozzle of the boom). Fig. 10 a, 10.b and 10.c show the volumetric fraction contributed by each nozzle to the deposited volumetric flowrate at $x = 1$, 3 and 5 m, respectively.

The first nozzle contributes 44% of the flowrate that is being deposited at 1 m, while the second nozzle contributes 18%. At that distance, the first 13 nozzles provide 95% of the deposited flowrate. For 3 m, the first and second nozzles contribute 19% and 14% to the deposited flowrate, respectively. In addition, the first 23 provide 95% of the total flowrate. When the distance is 5 m, the first and second nozzles accounts for 26% of the total flowrate at that location. The 95% of the deposited flowrate is provided by the first 26 nozzles of the boom. These results indicate that, as the distance increases, more nozzles contribute to the deposited flowrate and therefore the multiple nozzle approach is required for a good representation of the spray drift.

4. Conclusions

The developed model satisfactorily predicts the spray drift data reported by different authors and obtained for a great variety of climatic conditions, nozzles, spraying pressures, boom heights and a wide range of distances in the downwind direction. The results indicate that the dispersion phenomenon has to be accounted for in the model to predict the spray drift accurately for distances longer than around 2 m.

The eddy diffusivity, the single fitted parameter of the calibrated model, was adequately correlated as a function of the relative humidity. In the absence of dispersion-related data, the fitted equation can be used to fully predict the deposited spray drift from horizontal boom sprayers.

The number of nozzles has a strong influence in the spray quality prediction. The ratio between the boom and single nozzle spray drifts increases significatively as a function of the downwind distance. For example, for the studied case, the 95% of the total deposited flowrate at 1, 3 and 5 m is accounted for the contribution of 13, 23 and 26 nozzles.

Regarding computational efficiency, it was found that around 2 ms were needed to obtain the spray drift value at a given distance using a PC Intel Core i7 4790S 8 Gb of RAM. This time is increased by 1.5 times when a google cloud virtual machine (f1-micro virtual processor, 0.6 Gb of RAM) is used. Even though the code would need to be refined, the model looks like as suitable to be used on board sprayers for online spray drift predictions.

The proposed modeling approach provides a simple, accurate and computationally efficient tool to predict the droplets fate from horizontal boom sprayers. It can assist applicators to achieve high quality sprays, while minimizing agrochemicals deposition outside of the target application area.

Uncited references

; ; ; ; ; ; ; ; Renaudo, 2020; .

Declaration of competing interest

The authors declare that they have no known competing financial interests or personal relationships that could have appeared to influence the work reported in this paper.
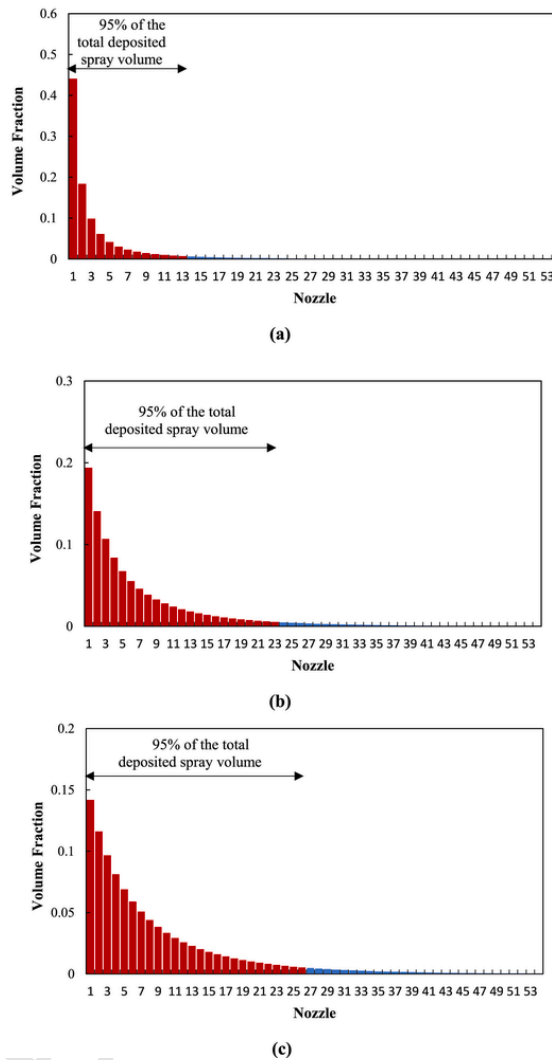
Fig. 10. Volumetric fraction contribution of each nozzle to the total deposited spray volume at: a) 1 m, b) 3 m and c) 5 m.

Data availability

Data will be made available on request.

Acknowledgments

Nomenclature

a_{ul}	Parameter defined in Equation (5) (−)
A_n	Nozzle orifice area (m²)
C_1	Parameter defined in Equation (36) (m⁻¹)
C_2	Parameter of Equation (37) (−)
C_d	Discharge coefficient (−)
d	Droplet diameter (m)
d_0	Atomized droplet diameter (m)
d_{crit}	Critical droplet diameter (m)

$d_{\max}$ Maximum diameter of atomized droplets (m)

$d_{\min}$ Minimum initial diameter of a droplet that reaches the soil surface (m)

D_{V10} Diameter where ten percent of the atomized droplets volume distribution has a smaller particle size (m)

D_{V50} Diameter where fifty percent of the atomized droplets volume distribution has a smaller particle size (m)

D_{V90} Diameter where ninety percent of the atomized droplets volume distribution has a smaller particle size (m)

D_Z Eddy diffusivity in the z coordinate (m^2/s)

f_d Density function of the atomized spray (1/m)

f_{x_0} Volume distribution pattern of atomized droplets (1/m)

$f_{d,x_0,x}$ Density function with respect to initial condition (d_0, x_0) and deposition distance x

f_{dx_0} Density function of the atomized spray with respect to d_0 and x_0/1/m)

f_{disp} Gaussian dispersion function (1/m)

f_x Density function of droplets with respect to the deposition distance for a nozzle (1/m)

f_x^{boom} Density function of droplets with respect to the deposition distance for a boom (1/m)

f_x^i Density function of droplets with respect to the deposition distance for the i-th nozzle (1/m)

F Desired applied dose (m^3/m^2)

g Gravity acceleration constant (m/s^2)

H Nozzle height (m)i Nozzle height (m)iNumber indicating the position of a nozzle on the boom (−)

k Constant defined in Equation (10) (s/m^2)

NNumber of nozzles on the boom (−)PAtomization pressure (Pa)Q Number of nozzles on the boom (−)PAtomization pressure (Pa)QNozzle volumetric flowrate for a nozzle (m^3/s)

Q^{boom} Nozzle volumetric flowrate for the boom (m^3/s)

RH Relative humidity (%)

s Spacing between nozzles on the boom (m)

t Time (s)

t_{dep} Deposition time of droplets (s)

t_{resp} Response time of a droplet (s)

T Wet bulb temperature (K)

T_{bh} Dry bulb temperature (K)

U Wind speed (m/s)

$\bar{U}$ Representative wind speed of the total atomized droplets population (m/s)

U_0 Wind speed at the nozzle height H (m/s)

v_A Sprayer forward speed (m/s)

v_T Terminal velocity (m/s)

x Spatial downwind coordinate (m)

x_0 Spatial position of the volume distribution pattern (m)

Y Spray drift (−)

z Spatial vertical coordinate (m)

$\bar{z}$ Vertical distance traveled by a droplet (m)

Greek Symbols

β Parameter of Equation (10) (s/m^2)

γ Wind speed constant (−)

ε Roughness of the terrain (m)

θ Spray angle (rad)

Δz Vertical distance from the mean trajectory (m)

$\Delta \rho$ Difference between the density of the droplet and that of the air (kg/m^3)

μ_g Air viscosity (Pa s)

ρ_d Droplet density (kg/m^3)

σ_s Standard deviation of f_{x_0} (m)

σ_{ul} Parameter defined in 4 (−)

σ_z Dispersion coefficient (m)

Subscripts

i Number indicating the position of a nozzle on the boom

Appendix A.

Response time of a droplet to fluid motion (t_{resp})

It is defined as the time that elapses from when the droplet leaves the nozzle until it begins to feel the effect of the wind. t_{resp} is calculated for Stokes regime as (Fritsching, 2016):

$$t_{resp} = \frac{\rho_d d_0{}^2}{18 \mu_g} \tag{A1}$$

Deposition time (t_{dep})

This time accounts for the travel duration of a droplet from the nozzle to the ground surface. To its calculation, it is required to relate the droplet flight time to the traveled vertical distance. From equations (9) and (12), the following expression can be obtained:

$$t = k d_0{}^2 \left[1 - \left(1 - \frac{54 \mu_g \bar{z}}{k d_0{}^4 \Delta \rho g} \right)^{\frac{1}{3}} \right] \tag{A2}$$

Considering $\bar{z} = H$ in equation (A2), t_{dep} becomes:

$$t_{dep} = k d_0{}^2 \left[1 - \left(1 - \frac{54 \mu_g H}{k d_0{}^4 \Delta \rho g} \right)^{\frac{1}{3}} \right] \tag{A3}$$

The critical diameter (Equation (14)) is obtained by equating the response and deposition times (equations A1 and A3, respectively).

References

Amsden, R.C. (1962). *Reducing the evaporation of sprays. Agricultural aviation, 4*(3), 88–93.

Bilanin, A.J., Teske, M.E., Barry, J.W., & Ekblad, R.B. (1989). *AGDISP: The aircraft spray dispersion model, code development and experimental validation. Transactions of the American Society of Agricultural Engineers, 32*(1), 327–334. https://doi.org/10.13031/2013.31005.

Bozon, N., Sinfort, C., & Mohammadi, B. (2009,). A GIS-based atmospheric dispersion model. *STIC & environnement* (p. 17). https://doi.org/10.3166/jesa.44.445-461.

Briggs, G.A. (1973). *Diffusion estimation for small emissions: Atmospheric turbulence and diffusion laboratory contribution file No. 79*. Oak Ridge, Tennessee: US National Oceanic and Atmospheric Administration (NOAA), Atmospheric Turbulence and Diffusion Laboratory.

Brugge, R. (1996). *Back to basics: Atmospheric stability: Part 1—basic concepts. Weather, 51*(4), 134–140.

Butler Ellis, M.C., & Miller, P.C.H. (2010). *The silsoe spray drift model: A model of spray drift for the assessment of non-target exposures to pesticides. Biosystems Engineering, 107*(3), 169–177. https://doi.org/10.1016/j.biosystemseng.2010.09.003.

De Visscher, A. (2013). *Air dispersion modeling: Foundations and applications.* John Wiley & Sons.

Finch, C.W., Byrne, T., Oloumi-Sadeghi, et al. (2014). *Liquid pesticide compositions.* United States Patent. Patent 8741324 B2.

Fritsching, U. (2016). *Process-spray: Functional particles produced in spray processes.* Springer.

Golder, D. (1972). *Relations among stability parameters in the surface layer. Boundary-Layer Meteorology, 3,* 47–58.

Holterman, H.J., van de Zande, J.C., Porskamp, H.A.J., & Huijsmans, J.F.M. (1997). *Modelling spray drift from boom sprayers. Computers and Electronics in Agriculture, 19*(1), 1–22. https://doi.org/10.1016/S0168-1699(97)00018-5.

Hong, S.W., Zhao, L., & Zhu, H. (2018). *SAAS, a computer program for estimating pesticide spray efficiency and drift of air-assisted pesticide applications. Computers and Electronics in Agriculture, 155,* 58–68. https://doi.org/10.1016/j.compag.2018.09.031.

Iturbide-Sanchez, F., da Silva, S.R.S., & Liu, Q. (2016,). Use of temperature and humidity profiles derived from satellite retrievals for the derivation of atmospheric stability indices. *2016 IEEE international geoscience and remote sensing symposium (IGARSS)* (pp. 3963–3966). IEEE.

Jacobson, M.Z. (2005). *Fundamentals of atmospheric modeling.* Cambridge university press.

Kayes, I., Shahriar, S.A., Hasan, K., Akhter, M., Kabir, M.M., & Salam, M.A. (2019). *The relationships between meteorological parameters and air pollutants in an urban environment. Global Journal of Environmental Science and Management, 5*(3), 265–278.

Lebeau, F., Verstraete, A., Stainier, C., & Destain, M.F. (2011). *RTDrift: A real time model for estimating spray drift from ground applications. Computers and Electronics in Agriculture, 77*(2), 161–174. https://doi.org/10.1016/j.compag.2011.04.009.

Leunda, P., Debouche, C., & Caussin, R. (1990). *Predicting the transverse volume distribution under an agricultural spray boom. Crop Protection, 9*(2), 111–114.

Liu, C.H., Mo, Z., & Wu, Z. (2018). *Parameterization of vertical dispersion coefficient over idealized rough surfaces in isothermal conditions. Geoscience Letters, 5*(1), 1–11.

Løfstrøm, P., Bruus, M., Andersen, H.V., Kjær, C., Nuyttens, D., & Astrup, P. (2013). *The OML-SprayDrift model for predicting pesticide drift and deposition from ground boom sprayers. Journal of Pesticide Science,* D12–D64. https://doi.org/10.1584/jpestics.D12-064.

Mawer, C.J., & Miller, P.C.H. (1989). *Effect of roll angle and nozzle spray pattern on the uniformity of spray volume distribution below a boom. Crop Protection, 8*(3), 217–222. https://doi.org/10.1016/0261-2194(89)90030-6.

Miller, P.C.H., & Hadfield, D.J. (1989). *A simulation model of the spray drift from hydraulic nozzles. Journal of Agricultural Engineering Research, 42*(2), 135–147. https://doi.org/10.1016/0021-8634(89)90046-2.

Murphy, S.D., Miller, P.C.H., & Parkin, C.S. (2000). *The effect of boom section and nozzle configuration on the risk of spray drift. Journal of Agricultural Engineering Research, 75*(2), 127–137.

Numpy. Last accessed on January 10, 2023 www.numpy.org.

Nuyttens, D. (2007). *Drift from field crop sprayers: The influence of spray application technology determined using indirect and direct drift assessment means.* Katholieke Universiteit Leuven. https://lirias.kuleuven.be/1714472.

Onorato, A., & Tesouro, M.O. (2006). *Pulverizaciones agrícolas terrestres* (1ra ed.). UNLP.

Pasquill, F. (1961). *The estimation of the dispersion of windborne material. The Meteorological Magazine, 90,* 20–49.

Post, S.L., Roten, R.L., & Connell, R.J. (2017). *Discharge coefficients of flat-fan nozzles. Transactions of the American Society of Agricultural and Biological Engineers, 60*(2), 347–351. https://doi.org/10.13031/trans.12064.

Pretty, J. (2008). *Agricultural sustainability: Concepts, principles and evidence. Philosophical Transactions of the Royal Society B: Biological Sciences*, *363*(1491), 447–465. https://doi.org/10.1098/rstb.2007.2163.

Pretty, J., & Bharucha, Z.P. (2014). *Sustainable intensification in agricultural systems. Annals of Botany*, *114*(8), 1571–1596. https://doi.org/10.1093/aob/mcu205.

Python. Last accessed on January 10, 2023 https://docs.python.org/3/library/timeit.html.

Renaudo, C.A. (2020). *Modelo predictivo de la deriva de pulverización en aplicaciones agrícolas de botalón*. Argentina: Universidad Nacional del Sur. Retrieved September 2, 2020, from: http://repositoriodigital.uns.edu.ar/handle/123456789/5147.

Renaudo, C.A., Bertin, D.E., & Bucalá, V. (2022). *A coupled atomization-spray drift model as online support tool for boom spray applications. Precision Agriculture*, 1–27. https://doi.org/10.1007/s11119-022-09923-1.

Richards, P.J., & Norris, S.E. (2011). *Appropriate boundary conditions for computational wind engineering models revisited. Journal of Wind Engineering and Industrial Aerodynamics*, *99*(4), 257–266.

Seinfeld, J.H., & Pandis, S.N. (2016). *Atmospheric chemistry and physics: From air pollution to climate change*. John Wiley & Sons.

Slade, D.H. (1968). *METEOROLOGY AND ATOMIC ENERGY, 1968 (No. TID-24190)*. Environmental Science Services Administration, Silver Spring, Md. Air Resources Labs.

Smith, D.B., Bode, L.E., & Gerard, P.D. (2000). *Predicting ground boom spray drift. Transactions of the ASAE*, *43*(3), 547. https://doi.org/10.13031/2013.2734.

Stainier, C., Robaye, V., Destain, M.F., Schiffers, B., & Lebeau, F. (2006). *Experimental evaluation of a spray drift Gaussian tilting plume model. Aspects of Applied Biology*, *77*(2), 365–370. Retrieved May 5, 2018 https://orbi.uliege.be/handle/2268/79232.

Stull, R. (2011). *Wet-bulb temperature from relative humidity and air temperature. Journal of Applied Meteorology and Climatology, 50*(11), 2267–2269.

Tan, Z. (2014). *Air pollution and greenhouse gases from basic concepts to engineering applications for air emission control*. Springer. https://doi.org/10.1007/978-981-287-212-8.

Tepper, G. (2012). *Weather essentials for pesticide application*. Grains Research & Development Corporation.

Teske, M.E., Miller, P.C.H., Thistle, H.W., & Birchfield, N.B. (2009). *Initial development and validation of a mechanist spray drift model for ground boom sprayers. Transactions of the American Society of Agricultural and Biological Engineers*, *52*(4), 1089–1097. https://doi.org/10.13031/2013.27779.

Teske, M.E., Thistle, H.W., Riley, C.M., & Hewitt, A.J. (2016). *Initial laboratory measurements of the evaporation rate of droplets inside a spray cloud. Transactions of the ASABE*, *59*(2), 487–493. https://doi.org/10.13031/trans.59.11543.

Teske, M.E., Thistle, H.W., Schou, W.C., Miller, P.C.H., Strager, J.M., Richardson, B., … Thompson, D.G. (2011). *A review of computer models for pesticide deposition prediction. Transactions of the ASABE*, *54*(3), 789–801. https://doi.org/10.13031/2013.37094.

Tieleman, H.W. (2003). *Roughness estimation for wind-load simulation experiments. Journal of Wind Engineering and Industrial Aerodynamics*, *91*(9), 1163–1173.

Turner, D.B. (1964). *A diffusion model for an urban area. Journal of Applied Meteorology and Climatology*, *3*(1), 83–91.

Venkatram, A. (1996). *An examination of the Pasquill-Gifford-Turner dispersion scheme. Atmospheric Environment*, *30*(8), 1283–1290.

van de Zande, J.C., Michielsen, J.G.P., Stallinga, H., & van Velde, P. (2014). Spray drift of reducing nozzle types spraying a bare soil surface with a boom sprayer. *International advances in pesticide application*: *Vol. 122* (pp. 245–254). Oxford, UK http://edepot.wur.nl/352735.

Zannetti, P. (2013). *Air pollution modeling: Theories, computational methods and available software*. Springer Science & Business Media.